DE GRUYTER
OPEN

Ekológia (Bratislava) Vol. 36, No. 1, p. 10–24, 2017
DOI:10.1515/eko-2017-0002

DISCRIMINATING SEDIMENT AND CLEAR WATER OVER CAOSTAL WATER USING GD TECHNIQUE

ABD RAHMAN MAT AMIN[1*], FADHLI AHMAD[2], KHIRUDDIN ABDULLAH[3]

[1]Faculty of Applied Sciences, Universiti Teknologi MARA, Kampus Kuala Terengganu, 21080 Kuala Terengganu, Malaysia; e-mail: abdra401@tganu.uitm.edu.my
[2] School of Ocean Engineering, Universiti Malaysia Terengganu, 21030 Kuala Terengganu, Terengganu, Malaysia
[3] School of Physics, Universiti Sains Malaysia, 11800 Minden, Pulau Pinang, Malaysia

* Author for correspondence

Abstract

Mat Amin A.R., Ahmad F., Abdullah K.: Discriminating sediment and clear water over coastal water using GD technique. Ekológia (Bratislava), Vol. 36, No. 1, p. 10–24, 2017.

Currently two algorithms are being used routinely by the MODIS Atmosphere and Ocean Team in order to distinguish sediment influence and clear water pixels over turbid water area. These two algorithms require complicated computational analyses. In this paper, a simple algorithm based on empirical technique to detect the sediment-influenced pixels over coastal waters is proposed as an alternative to these two algorithms. This study used apparent reflectance acquired from MODIS L1B product. This algorithm is based on the gradient difference of the line connecting the 0.47- and 1.24-μm channels and 0.47- and 0.66-μm channels of a log–log graph of the apparent reflectance values against MODIS wavelengths. Over clear-water areas (deep blue sea), the 0.47-, 0.66- and 1.24-μm channels fitted very well in line with correlation $R > 0.99$. Over turbid waters, a substantial increase of 0.66 μm in the reflectance leads to a low correlation value. By computing the difference between the gradient of the line connecting 0.47 and 0.66 μm and the gradient of the line connecting 0.47 and 1.24 μm, the threshold to discriminate turbid and shallow coastal waters from clear-water pixels can be obtained. If the gradient difference is greater than 0, the pixels were then marked as sediment-influenced pixels. This proposed algorithm works well for MODIS Terra and Aqua sensor. The comparison of this algorithm with an established algorithm also showed a good agreement.

Key words: MODIS; sediment; coastal water; turbid.

Introduction

The main objective of this study is to develop an alternative algorithm based on empirical technique to determine the sediment-influenced area along coastal waterlines using MODIS land channels. The distribution patterns of sediments play an important role in monitoring marine environmental changes, especially in coastal areas (Min et al., 2012). High concentration of suspended sediments along coastal waters and estuaries could affect the water columns and benthic processes (Miller, McKee, 2004) and will also reduce the underwater vertical transmit-

tance and phytoplankton productivity (May et al., 2003). Suspended sediments may also affect the nutrient dynamics (Mayer et al., 1998) and pollutant movement (Olsen et al., 1982). Over very high turbid water region such as Gulf of Martaban, the edge of the highly turbid zone found that mostly, the influence by the sediment could migrate back and forth with every tidal cycle by about 150 km (Ramaswamy et al., 2004). In order to study about the tidal or sea current influence on the sediment distribution and dispersal, the exact sediment location should be determined. Owing to the dynamic movement of the sediment influence zone, it is impossible to monitor this movement by using traditional ways such as water sampling. Alternatively, the daily sediment influence region is mapped and then compared. This goal can be achieved by exactly mapping and locating the spatial and temporal sediment distribution.

Numbers of studies have been conducted over water regions in order (Miller, McKee, 2004) to clearly distinguish sediment-influenced areas and clear-water areas and also to improve the atmospheric correction algorithm over water regions. Li et al. (2003) have developed an algorithm based on the empirical technique to detect the sediment-dominated waters by using MODIS Terra measurements at the visible and near-infrared (NIR) wavelengths. This developed algorithm used a regression technique (hereafter denoted as RT) that involves linear regression between the log of apparent reflectance (r[l]) and the log of wavelength (l) at 0.47, 1.24, 1.64 and 2.13 μm, respectively. This algorithm is currently being used as a routine in the MODIS Atmosphere Team to mask the sediment-influenced pixels over turbid coastal water (Levy et al., 2009). In order to remove the effect of sediments in the SeaWiFS imagery to improve chlorophyll product, Figueras et al. (2004) have proposed an algorithm that is based on a null point at 497 nm (corresponding to SeaWiFS band 4, cantered at 510 nm), where the level of reflectance is not affected by a change in chlorophyll concentration. Shi and Wang (2007) used the combinations of MODIS Aqua measured radiances at the short visible, NIR and shortwave infrared (SWIR) bands to detect the sediment-influenced area over MODIS imagery. Turbid water indexes (T_{ind}) of 748 and 1,240 nm have been proposed. This algorithm currently is used in the SeaWiFS Data Analysis System (SeaDAS). However, Morel and Belanger (2006) have refined the scheme using the normalised water-leaving radiance (nLw[λ]) threshold value at the green band for turbid water detection. Recently, Matsushita et al. (2012) have proposed a new method to distinguish Case 1 and Case 2 waters over ocean regions. The method uses remote-sensing reflectance (R_{rs}) of 412 and 443 nm, respectively.

The above discussion shows that several algorithms have been used to discriminate turbid and clear waters in remote sensing images. However, the proposed algorithms are computationally complex. In order to reduce the processing step and simplify the computation, a new and simple algorithm based on the empirical technique to detect and map the sediment-influenced pixels in the MODIS imagery along coastal water is proposed. The same MODIS product (L1B) is used in the development of RT and normalised difference vegetation index (NDVI) algorithms. Although the RT algorithm did not use atmospheric corrected product, the algorithms have found to be very effective to discriminate sediment and clear water over ocean region. The proposed algorithm is based on the difference in the gradient of the line connecting the 0.47- and 1.24-μm (0.47:1.24) channels and the 0.47- and 0.66-μm (0.47:0.66) channels of a log–log graph of the reflectance values against their MODIS Terra wavelengths. By subtracting the gradient of the line connecting 0.47 and 0.66 μm from the gradient of the line connecting 0.47 and

1.24 μm, the threshold value to discriminate turbid and shallow coastal waters from clear water pixels can be obtained. The results of this algorithm are then evaluated by comparing each masked area with the corresponding masks generated by using another established technique.

Data and study area

This algorithm used spectral reflectance acquired from MODIS L1B data. This product is used as a main data. MODIS L1B is calibrated reflectance product provided by the MODIS Characterisation Support Team (MCST). The spectral 'reflectance' (r_l) is defined as a function of the measured spectral radiance (L_λ), the solar zenith angle (θ_0) and the solar irradiance (F_0) in the wavelength band λ (Levy et al., 2009):

$$\rho_\lambda = L_\lambda \frac{\pi}{F_{0,\lambda} \cos(\theta_0)} \qquad (1)$$

The data is downloaded from MODIS Level 1 and Atmosphere Archive and Distribution System (LAADS) website. This data is used to develop the Gradient Different - GD, RT and T_{ind} algorithms. There were two types of MODIS L1B data used in this study. The two data, MOD021KM and MYD021KM, are used to derive an algorithm for Terra and Aqua sensor, respectively. Another data called geolocation product (MOD03) is used as a supplementary data to the T_{ind} algorithm. Numbers of data have been tested during this study. However, in this paper, only four images are used as examples to represent the ability of the algorithm. The study has been conducted over numerous MODIS datasets acquired from different geographical region. Images used in this study was well selected to ensure that all parameter especially sediment are available in the images. The areas have been chosen because numbers of researcher have used them as their areas of study.

Development of the empirical algorithm and methodology

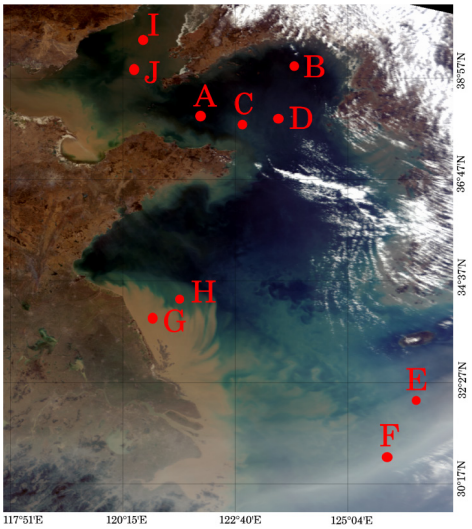

Fig. 1. MODIS true colour image (red: 0.66 μm, green: 0.55 μm, blue: 0.47 μm) acquired from MODIS Terra over the east coastal areas of China at UTC 02:45 on 9 February 2004. The image shows low sediment, high sediment and varying amount of pollution aerosol marked as A–J.

Development of the Empirical Algorithm

In this study, a true colour image (red: 0.66 μm, green: 0.55 μm, blue: 0.47 μm) of a MODIS Terra scene acquired over the east coastal area of China at UTC 02:45 on 9 February 2004, as shown in Fig. 1, is used as a training field.

Based on the visual inspection, areas A–F are less turbid and referred to as clear water areas. Areas G–J are visually turbid water areas with significant suspended sediments. Aerosol concentration over the training area is obtained by comparing this image with the aerosol optical depth (AOD) map acquired from MODIS aerosol product (MOD04). According to the MOD04 product, the AOD for point A–F is 0.144, 0.170, 0.231, 0.234, 0.444 and 0.883, respectively. However, no AOD value is obtained over point G–I. In the MOD04 product, these points are masked because of the presence of sediment.

In order to have more understanding about the reflectance properties over clear and sediment-influenced areas, a log–log graph of reflectance against wavelength has been plotted. Figure 2 shows the plotted for a clear water area with a high aerosol concentration (F) and turbid water with significant sediment contribution (G) on the log–log scale plot. Over clear water area, the linear regression of the reflectance of the 0.47-, 0.55-, 0.66-,

0.87-, 1.24-, 1.64-, and 2.13-μm channels against wavelength shows very high correlation, greater than 0.99. Meanwhile, over sediment-influenced area (G), there are significant increment in 0.55-, 0.66- and 0.87-μm channels. The increments in these channels decreased the correlation coefficient of the line connecting the 0.47, 0.55, 0.66, 0.87, 1.24, 1.64 and 2.13 μm, significantly. Detailed discussion on the clear water, sediment and aerosol apparent reflectance can be found in Li et al. (2003).

Detailed observation of Fig. 2 shows that a straight line can be drawn to fit the 0.47-, 1.24-, 1.64- and 2.13-μm channels for either clear water or sediment-influenced areas. It means that the gradient of the line connecting 0.47 μm with any of these three channels (1.24, 1.64 and 2.13 μm) can be used instead of the regression line connecting all of the channels (0.47, 1.24, 1.64 and 2.13 μm). Meanwhile, over the sediment-influenced area, the gradient of the line connecting the 0.47-μm channel with any of the three channels (0.55, 0.66 and 0.87 μm) decreased gradually. So the difference in the gradient can be used as an indicator to separate sediments and clear water areas over ocean regions.

As mentioned earlier, there are three channels that are influenced by the sediments (0.55, 0.66 and 0.87 μm). In this study, the reflectance of the 0.66-μm channel is chosen to be paired with the 0.47-μm channel. The 0.66-μm channel has been chosen because the 0.55-μm channel is being influenced more by bottom effects (Li et al., 2003). Meanwhile the 0.87-μm channel comparatively produced a lower signal from sediments. As stated before, the linear relationship of the line connecting the 0.47-, 1.24-, 1.64- and 2.13-μm channels was not influenced by the sediment and aerosol. The lines connecting these channels were fitted very well with the power law formula over sediment, clear water and aerosol contribution area. There are three

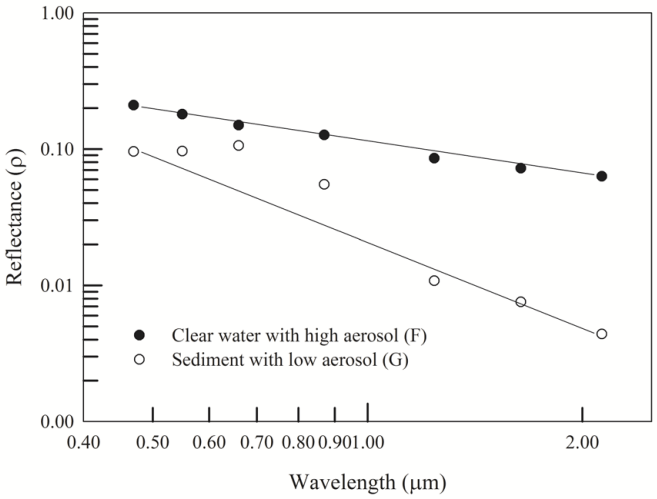

Fig. 2. Graph of reflectance against wavelength for clear water with high aerosol concentration (F) and sediment influence region with low aerosol concentration (G) on log–log scale.

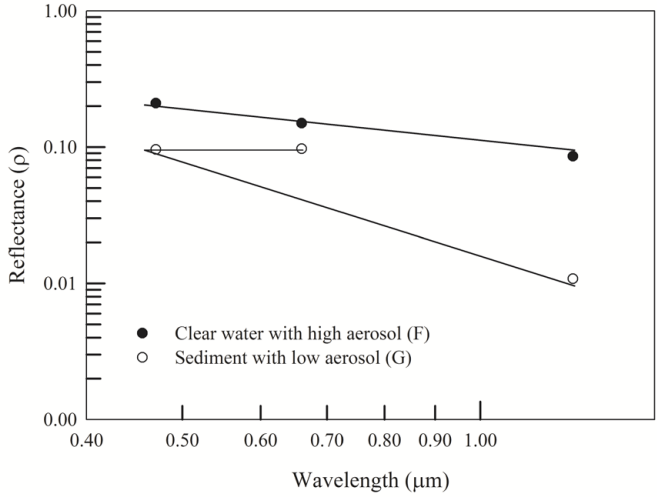

Fig. 3. Log–log plot of gradient line for clear water area with high aerosol concentration (F) and sediment-influenced area with low aerosol concentration (G).

channels that could be paired with the 0.47-μm channel. However, it is well known that the 1.64 μm (channel 6) of MODIS Aqua is not functional since their launch. It is because 15 out of 20 of the accompanying detectors are non-functional (Salomonson et al., 2006). Furthermore, the 2.13-μm channel of Terra sensor is subject to data dropouts because of an instrument crosstalk issue (Aurin et al., 2013). The only channel left is 1.24 μm. So in this study, the 1.24-μm channel is used to pair with the 0.47-μm channel.

Figure 3 shows the difference in the gradient for the line connecting the 0.47:0.66 μm channels for the clear water and sediment-influenced areas. For the sediment-influenced area, the gradient of the line connecting the 0.47:0.66 μm channels is lower than that connecting the 0.47:1.24 μm channels. Meanwhile, over clear water areas, the gradient of the line connecting the 0.47:0.66 μm channels is almost the same with that connecting the 0.47:1.24 μm channels. So, the decrease in the gradient of the 0.47:0.66 μm lines over the sediment-influenced area is only due to the contribution of sediment reflectance.

In this study, a simple method based on the gradient difference, Δm, for the line connecting the 0.47:0.66 μm channels (m_1) and the line connecting the 0.47:1.24 μm channels (m_2) is proposed. The algorithm is given by the following equations:

$$m_1 = \frac{\log_{10}(\rho_{0.66}) - \log_{10}(\rho_{0.47})}{\log_{10}(\lambda_{0.66}) - \log_{10}(\lambda_{0.47})} \quad (2)$$

$$m_2 = \frac{\log_{10}(\rho_{1.24}) - \log_{10}(\rho_{0.47})}{\log_{10}(\lambda_{1.24}) - \log_{10}(\lambda_{0.47})} \quad (3)$$

$$\Delta m = m_1 - m_2 \quad (4)$$

where $l_{0.47}$, $l_{0.66}$, $l_{1.24}$ and $r_{0.47}$, $r_{0.66}$, $r_{1.24}$ are the wavelengths and apparent reflectance of the MODIS 0.47-, 0.66-, and 1.24-μm channels, respectively.

Methodology

This study was conducted as follows. First, MODIS L1 data is downloaded. The derived data was processed by using ENVI 4.5 software. The data was then converted to PCI Geomatica file for further analyses. The converted data was then masked to remove the presence of land in the image. This procedure is necessary because the intention of this study is to detect the presence of sediments over turbid water areas. This procedure was achieved by applying an NDVI-like algorithm that is very effective to discriminate land and water bodies (Levy et al., 2009). If the NDVI value is greater than 0.1, the pixel is considered as water. A simple clouds masking technique is applied to remove the presence of clouds over the study area. Single reflectance of 0.87-μm channel ($r_{0.87}$) and the ratio of 0.87-μm to 0.66-μm channel ($r_{0.86}/r_{0.65}$) are used in this study (Ackerman et al., 2010). After the land and clouds that covered the areas have been masked, the GD algorithm is then applied.

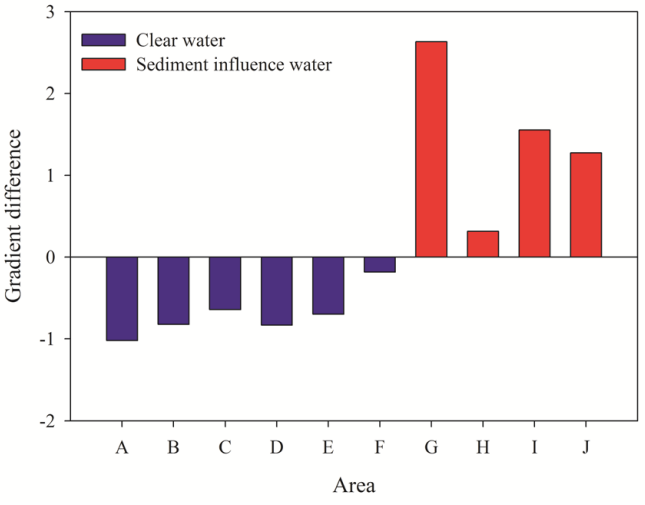

Fig. 4. The gradient difference as a function of clear water area (A–F) and sediment influence area (G–J) as marked in Fig. 1.

Figure 4 shows the plotted GD against the study area condition. Based on the graph, the variation of GD is depending on the water composition. Over clear water areas, the GD algorithm shows the low value. The GD value is still negative even over very high aerosol concentration area (F). However, the GD values increased drastically over the sediment-influenced areas (area G, H, I, and J). This figure shows that even no atmospheric correction is applied to the data, the sediment and clear water region can be easily differentiated. The results also shows that the GD values over sediment-influenced area are not depend on the aerosol concentration and always in positive value. Meanwhile, the GD values over clear water are always negative. In this study, pixels with GD values greater than 0 were marked as sediment-influenced pixels.

Accuracy

The accuracy of the proposed algorithm is the most important issue. In this study, the RT and T_{ind} map is assumed as a reference map. To access the accuracy of the GD map that was developed by using MODIS Terra images, it was validated with the RT map that was developed by using the same sensor. Meanwhile, the accuracy of GD map that was developed by using MODIS Aqua image has been validated with the T_{ind} map. The accuracy assessment is conducted as follow. First, the map for the GD, RT and T_{ind} is generated based on their respective algorithm. In each map, the sediment influence pixel is being classified as 1, meanwhile the clear water pixel is being classified as 2. Second, the comparison map is plotted. In this step, the map is then compared according to pixels by pixels. The same pixels detected as sediment by both algorithm is classified as 11. The pixels detected as sediment by RT or T_{ind} algorithm but detected as clear water by GD algorithm is classified as 12. The pixels detected as clear by T_{ind} or RT but as sediment by GD are classified as 21. After that, the number of pixels in each class is then calculated. The detail notation and the colour code used for each class are given below. After the pixels were calculated, the error matrix table (Table 1) is then constructed. The numbers of pixels for each class is then placed into the table. Lastly, the commission error, omission error, user accuracy and producer accuracy are then calculated. In order to have better understanding of the calculation used in this study, Fig. 5(d) is referred. The percentage of user accuracy is calculated as the number of red pixels divided by the total number of red and green pixels. The percentage of producer accuracy is defined as the number red pixels divided by the total number of red and orange pixels. Meanwhile, the commission sediment percentage is the number of green pixels divided by the total number of red and green pixel. The omission sediment is defined as the ratio of orange pixels to the total number of red and orange pixel. Overall accuracy is the ratio of total number of red and blue pixels to the total number of blue, red, green and orange pixels.

T a b l e 1. Error matrix.

	1	2	
1	N_{11}	N_{21}	$N_{11}+N_{21}$
2	N_{12}	N_{22}	$N_{12}+N_{22}$
	$N_{11}+N_{12}$	$N_{21}+N_{22}$	$N_{11}+N_{22}$

N_{11} (Red) = number of same pixels detected as sediment by GD and RT or T_{ind}.
N_{21} (Green) = number of sediment pixels detected by GD but as clear water by RT or T_{ind}.
N_{12} (Orange) = number of pixels detected as clear water by GD but as sediment by RT or T_{ind}.
N_{22} (Blue) = number of same pixels detected as clear water by GD and RT or T_{ind}.

Results and discussion

The empirical algorithm mentioned above was tested over numerous MODIS datasets. This section represents the samples result of the GD algorithm, RT, T_{ind} and also the comparison map.

Aqua Sensor Sample Images

The results for sample images acquired from MODIS Aqua over Chesapeake Bay at UTC 18:20 on 5 April 2004 and China Sea at UTC 05:15 on 19 October 2003 are describes in the following text.

Chesapeake Bay

Figure 5(a) shows a true colour image of the MODIS scene acquired from MODIS Aqua instrument over the Chesapeake Bay and nearby area at UTC 18:20 on 5 April 2004. The image

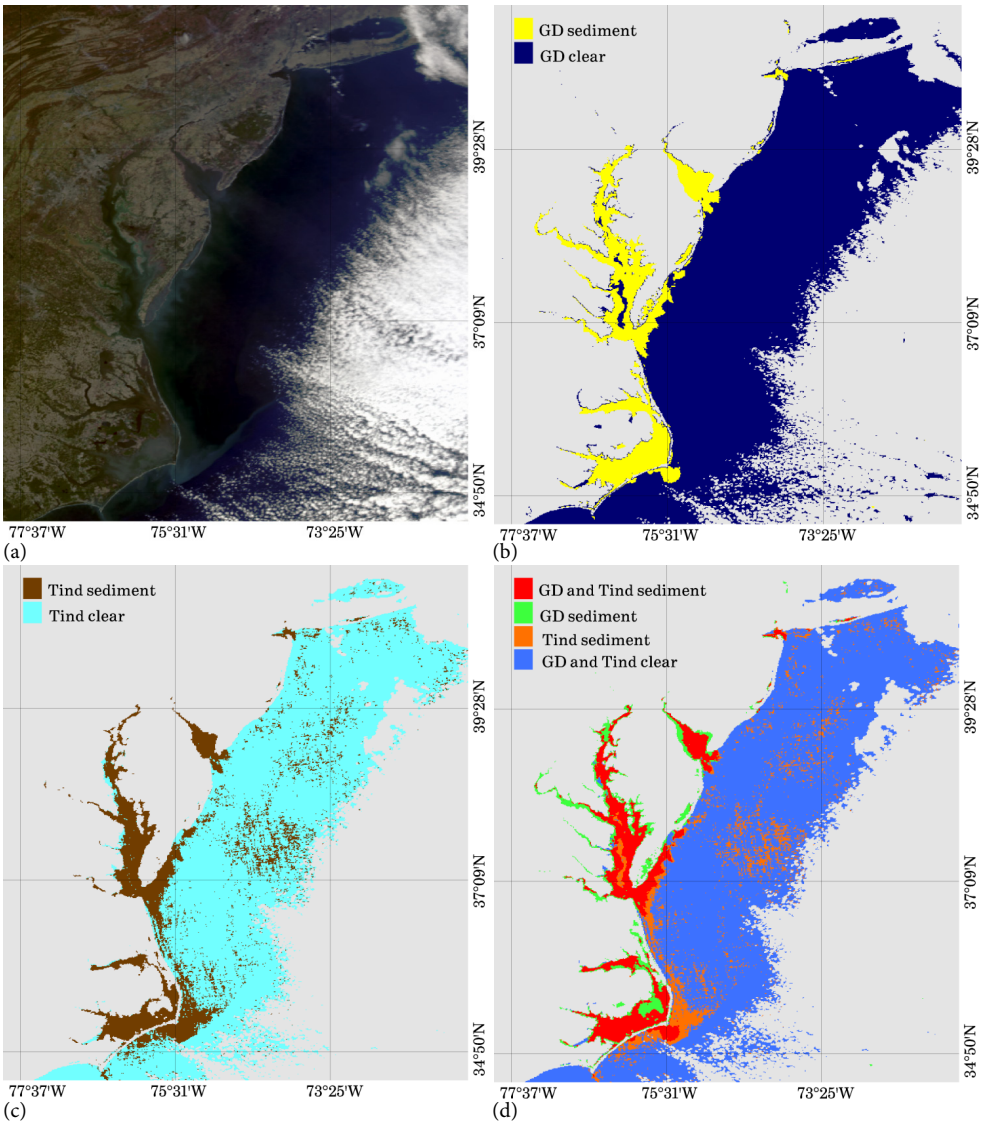

Fig. 5. (a) Colour images (red: 0.66 μm; green: 0.55 μm; blue: 0.47 μm) acquired from MODIS Aqua over the Chesapeake Bay and nearby area at UTC 18:20 on 5 April 2004; (b) the result of GD technique; (c) the result of T_{ind}; (d) comparison of the GD and T_{ind} algorithm.

covers approximately the latitude range of 34°N–41°N and the longitude range of 71°E–77°W. Significant amount of sediment can be seen clearly at the estuaries area and at the bottom of the image.

Figure 5(b) shows the result of the GD algorithm applied over the area. In this figure, the sediment-influenced regions that were represented by the brownish colour along the shore line are successfully mapped as shown by the yellow colour. The brownish colours that located over the river mouth were also detected successfully. There were no sediment pixels detected at the right portion of the image. The result shows that the sediment influence region is located near to the land. Figure 5(c) shows the result of T_{ind} algorithm that applied over the same scene. The masked pixels are represented by the dark brown colour. This algorithm successfully detects the sediment pixels along the river, over the river mouth and along the coastal line. Numbers of pixels that was located at the right portion of this image is masked as sediment pixels. The comparison map of the GD and T_{ind} algorithm is shown in Fig. 5(d). In this map, the same pixel detected by both algorithms is represented by red colour. Most red colour pixels are located over the highly turbid water that represented by brownish colour as seen in Fig. 5(a). Commission pixels for sediment class are represented by green colour. These pixels are mostly located along coastal line and highly turbid river bank (Fig. 5(d)). The omission pixels represented by the orange colour are mostly located over the deeper water region.

China East Coastal

Figure 6(a) shows a colour image of the MODIS scene acquired from MODIS Aqua instrument over the China Sea and nearby areas at UTC 05:15 on 19 October 2003. The image covers approximately the latitude range of 29°N–31°N and the longitude range of 119°E– 124°E. At the right corner of this image is the East China Sea. Yangtze River that is the longest river in the Asia can be clearly seen in this image. Large region of sediment can be seen along the coastal line and over the river mouth.

Figure 6(b) shows the result of the GD algorithm that has been applied over this area. The sediment pixels detected by this algorithm is represented by yellow colour. Uniform yellow colour can be observed in this figure. The uniform dark blue colour over the right corner of this image indicated that no sediment pixels detected over this region. The sediment pixels that are detected by the T_{ind} algorithm are shown by the dark brown colour in Fig. 6(c). In this figure, no sediment influence pixels are detected along the river and over the highly turbid river mouth. This is due to the saturation of the 748-nm channel that is used in the T_{ind} algorithm (Aurin et al., 2013). However, as compared to the GD algorithm, a significant numbers of sediment-influenced pixels are detected by this algorithm over the blue water region, as shown in Fig. 6(a).

Figure 6(d) shows the comparison map of the GD and T_{ind} algorithm over the study area. The red colour is clearly seen near the shore line and over the river mouth. The green colour that represents the sediment pixels detected only by GD algorithm is located along the shoreline, over the river mouths and along the river. According to Fig. 6(a), this region is sediment-dominated area, which represented by the brownish colour. Although this region appears to be highly turbid, the presence of the sediment is still detected by the GD algo-

rithm. However, no data recorded by T_{ind} over this green region. Obvious number of orange pixels is scattered over the edge of turbidity zone and the deeper water region. Over the edge of the turbidity zone, the GD shows negative values. Although this region appears turbid with greenish to bluish colour, no sediment is detected. The bluish or greenish colour could represent the phytoplankton-dominated area.

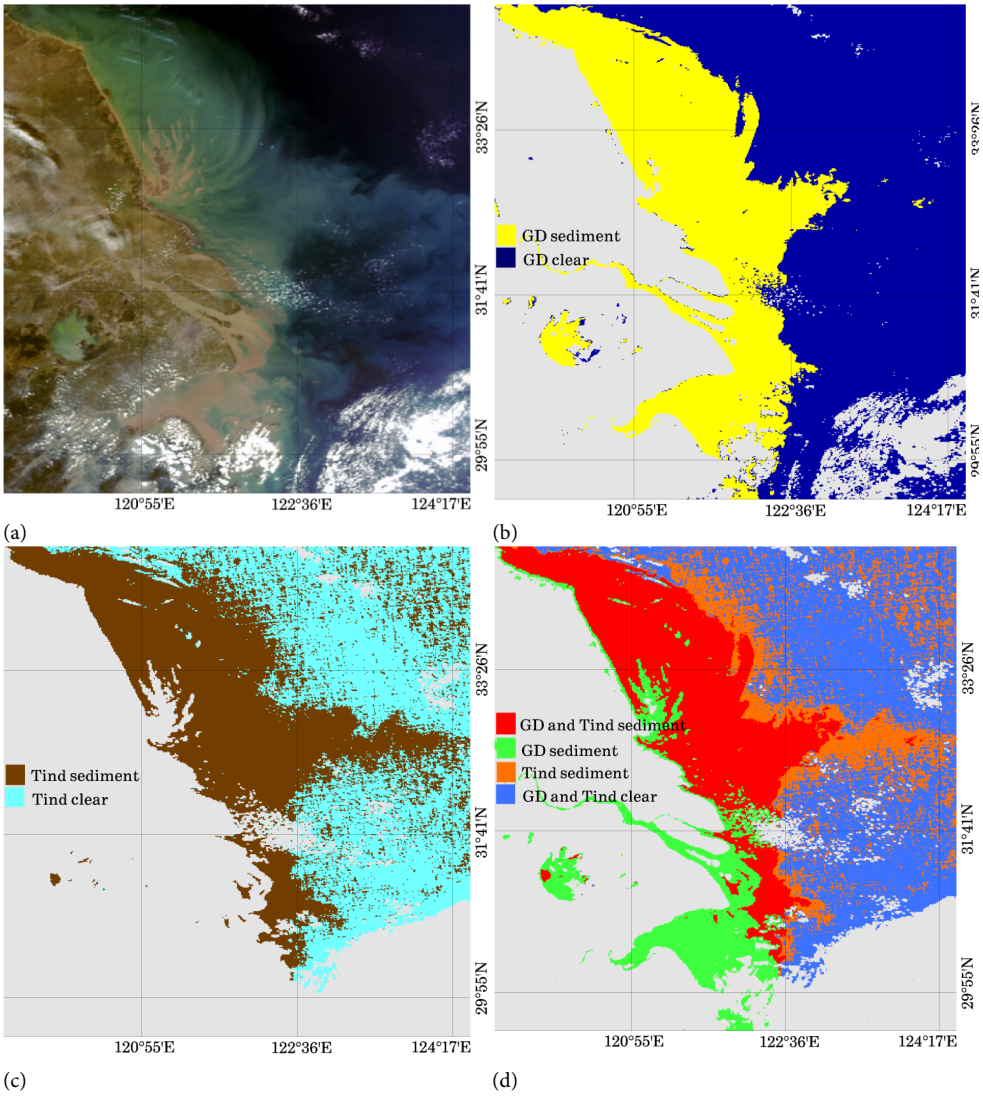

Fig. 6. (a) Colour images (red: 0.66 μm; green: 0.55 μm; blue: 0.47 μm) acquired from MODIS aqua instrument over the China Sea at UTC 05:15 on 19 October 2003; (b) the result of GD technique; (c) the result of T_{ind}; (d) comparison of the GD and T_{ind} algorithm.

Terra Sensor Sample Images

This section discussed the sample result for the dataset acquired from MODIS Terra over the Florida Peninsular at UTC 16:40 on 7 March 2001 and Gulf of Mexico at UTC 16:40 on 6 March 2013.

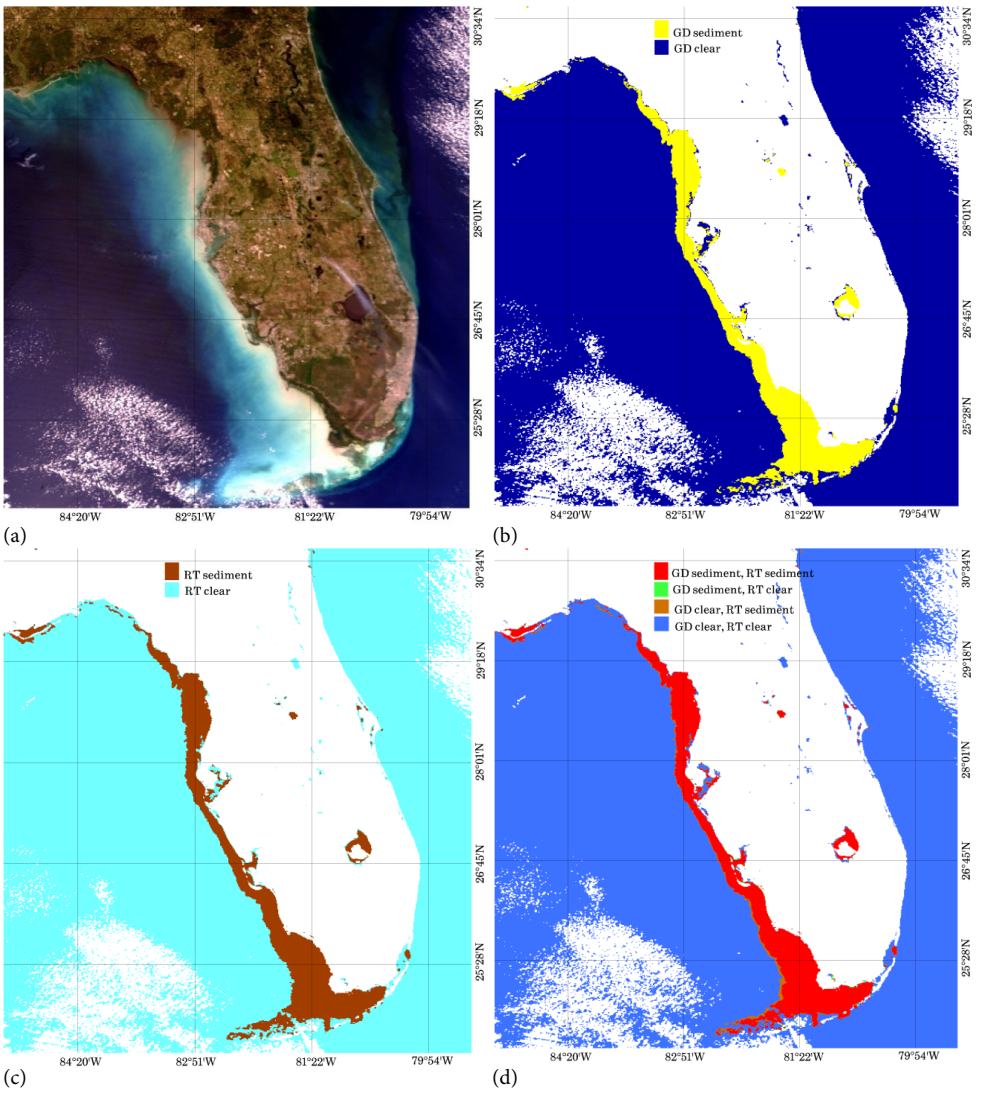

Fig. 7. (a) Colour images (red: 0.66 µm; green: 0.55 µm; blue: 0.47 µm) over the Florida peninsular at UTC 16:40 on 7 March 2001; (b) the result of GD technique; (c) the result of RT; (d) comparison of the GD and RT algorithm.

Coast of Florida

Figure 7(a) shows the true colour image of south eastern part of the United State. This area covers the Florida Peninsular and its nearby area. The figure covers roughly latitude range of 24°–30° N and longitude range of 79°–85°W. This image acquired from MODIS Terra at UTC 16:40 on 7 March 2001. Figure 7(b) shows the result of GD algorithm applied over the study area. In this image, large portion of sediment that are visible at the west side of Florida Peninsular are successfully masked. The Okeechobee Lake influenced by sediment is also successfully picked out. Figure 7(c) shows the result of the RT applied over the study area. Figure 7(d) shows the comparison of the GD and RT. Large portion of red colour that represent the same region that successfully masked by both algorithms.

Gulf of Mexico

Figure 8(a) shows the true colour image acquired from MODIS Terra on 6 March 2003 over the southern part of the United State and the Gulf of Mexico. Laden of sediment was clearly visible along the coastal line and the Mississippi River mouth at the lower portion of the image. Figure 8(b) shows the sediment that is successfully masked by the GD. Figure 8(c) represents the result of the RT algorithm. As a comparison, Fig. 8(d) is constructed. There are no significant different between these two algorithm. The green colour seen over the turbidity zone shows the excess sediment masked by the GD algorithm.

Accuracy

Table 2 shows the result of the accuracy assessment that has been conducted in this study for Terra and Aqua imagery. The result of the accuracy assessment conducted for Aqua sensor is shown in the upper part of Table 2. Over the Chesapeake Bay area, the user accuracy percentage for the sediment is 67.3%. The user accuracy percentage for China Sea is 67.8%. The percentage of commission error for the Aqua sensor is 32.7 and 32.2% for Chesapeake and China Sea, respectively. The higher in the commission percentage for the Chesapeake Bay is due to the numbers of pixels detected by the GD as sediment near the river bank and coastal line was classified as clear water by the T_{ind}. Over the China Sea, the majority of commission pixels were located along the river and coastal line as indicated by the green colour. The higher percentages of commission error are due to the saturation of the 748-nm channel used in the T_{ind} algorithm. Meanwhile, the producer accuracy for these sample images is 51.9 and 60.8%, respectively. The percentage of omission error is 48.1 and 39.2%. The lower producer accuracy and higher omission percentage for the Chesapeake Bay and China Sea are mostly due to the numbers of sediment pixels detected by the T_{ind} algorithm that is located far from the shore line as shown by the brown colour in Figs. 5(d) and 6(d). This area is considered as clear water in the true colour image as shown in Figs. 5(a) and 6(a). However, the GD algorithm has detected this area as clear water.

The result of the sediment accuracy assessment for the Terra images is shown in the lower part of Table 2. The user accuracy percentage for the Florida Peninsular and Gulf of Mexico

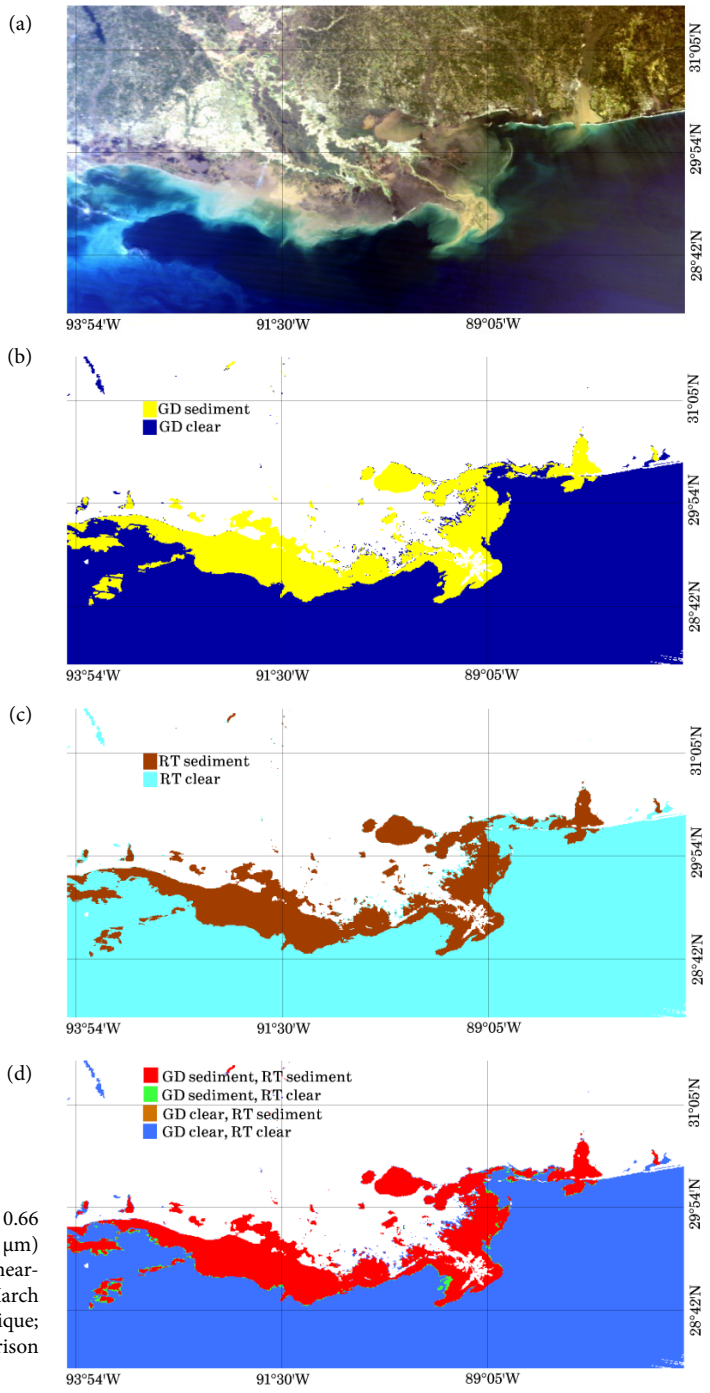

Fig. 8. (a) Colour images (red: 0.66 μm; green: 0.55 μm; blue: 0.47 μm) over the Gulf of Mexico and nearby areas at UTC 16:40 on 6 March 2013; (b) the result of GD technique; (c) the result of RT; (d) comparison of the GD and RT algorithm.

T a b l e 2. Accuracy assessment.

Sensor	Location	Class	User accuracy (%)	Commission (%)	Producer accuracy (%)	Omission (%)	Overall accuracy (%)
Aqua	Chesapeake	Sediment	67.3	32.7	51.9	48.1	75.4
		Clear	76.6	23.4	99.3	0.7	
	China sea	Sediment	67.8	32.2	60.8	39.2	62.5
		Clear	59.5	40.5	99.6	0.4	
Terra	Florida	Sediment	98.5	1.5	92.5	7.5	99.3
		Clear	99.3	0.7	99.9	0.1	
	Gulf of Mexico	Sediment	95.4	4.6	100	0	99.0
		Clear	100	0	98.8	1.2	

is 98.5 and 95.4%, respectively. The commission error percentage for the above mentioned images are 1.5 and 4.6%, respectively. The commission pixels are almost located along the coastal line and rivers bank. The producer accuracy percentage for the Terra images is given by 92.5 and 100.0%, respectively. Meanwhile, the omission error percentage is 7.5 and 0% respectively. Overall, the comparison between GD and RT shows better agreement as compared to GD and T_{ind}. The GD and RT also show good agreement in the clear water detection. The user and producer accuracy percentage is higher than 95%.

The above result shows that the GD, T_{ind} and RT algorithms agree that the sediment-influenced regions are located near to the coastal. The main different between GD and T_{ind} is in the detection of sediment over deep water region. Numbers of region detected by T_{ind} is scattered over the open water, whereas this region is represented by the blue colour in the true colour image. The other disagreement between these two algorithms is over the turbidity edge. Most of the regions classified as sediment by the T_{ind} are shown by the bluish to greenish colour in the true colour image that could represent the phytoplankton-dominated area. Furthermore, the saturation of the 748 nm over highly turbid water could limit the ability of the T_{ind} algorithm along the river and coastal line. However, the GD and RT algorithms are in high correlation for every scene. The ability of these two algorithms over deep water and along the coastal line is almost the same.

Conclusion

A simple algorithm using empirical technique to retrieve sediment-influenced pixels in MODIS imageries is proposed. This algorithm used MODIS land channels in the visible and NIR region. This method has been tested on carefully selected MODIS images acquired over different geographical regions. There are numbers of algorithms that have been proposed to detect and mask sediment-influenced pixels in MODIS images; however, these require more complicated computations compared to this proposed GD technique. The major contribution of the proposed GD technique is that this technique is simpler and faster than others algorithm. As an example, by using RT, the contribution from sediments at the 0.66 and 0.55 μm wavelengths are determined from the residuals/deviations from the regression line.

But by using the GD technique, the contribution of sediments was determined from the difference in the gradient lines. This proposed technique just involves the calculation of the difference in gradients and application of the selected threshold. Therefore, the computation for the gradient technique is simpler and faster than using the regression technique. Furthermore, the algorithm can be applied to the raw L1B and no atmospheric correction is required. Although this proposed algorithm only used L1B product and simple empirical method, sediment, clear water and dust could be differentiate from the plot and histogram. Consistent results were obtained when this algorithm is applied over different geographical region. The ability of this new proposed method is almost equivalent with RT and T_{ind} algorithm.

The results of the accuracy assessment indicated that the performance of the GD algorithm is comparable to that of the RT algorithm in each of the tested study areas, located in different geographical regions. Although this proposed algorithm is simpler and faster than RT, the agreement between GD and RT is higher for each case. Therefore, this new algorithm is a universal one, which can be applied to MODIS Terra data. In some cases, the area that detected as sediment influence by GD algorithm but not detected as sediment influence by others algorithm and vice versa. However, for the Aqua images, the accuracy percentage is quite low. The omission and commission percentage is quite high. The main reason for this result is the disagreement of these two algorithms to class the pixels that are located far from the coastal line. Numbers of these pixels is classed as sediment by the T_{ind}. However, the GD algorithm classes these pixels as a clear water pixels. On the other hand, the ability of these two algorithms to detect the sediment-influenced pixels over turbid water is almost the same. As a main conclusion, the proposed GD algorithm is recommended to use as an alternative algorithm to detect the sediment-influenced pixels over turbid water area for MODIS Terra and Aqua images.

Acknowledgements

We would like to thank the UiTM Kuala Terengganu, UMT and USM managements for their support and encouragement. Our appreciation also goes to the MODIS team for all the valuable data provided. We thank the reviewers and associate editor for their comments that improved this manuscript.

References

Ackerman, S., Strabala, K., Menzel, P., Frey, R., Moeller, C. & Gumley L. (2010). *Discriminating clear-sky from cloud with MODIS algorithm theoretical basis document (MOD35)*. Wisconsin: MODIS Cloud Mask Team, Cooperative Institute for Meteorological Satellite Studies, University of Wisconsin.

Aurin, D., Mannino, A. & Franz B. (2013). Spatially resolving ocean color and sediment dispersion in river plumes, coastal systems, and continental shelf waters. *Remote Sens. Environ.,* 137, 212–225. DOI:10.1016/j.rse.2013.06.018.

Figueras, D., Karnieli, A., Brenner, A. & Kaufman Y.J. (2004). Masking turbid water in the southeastern Mediterranean Sea utilizing the SeaWiFS 510 nm spectral band. *Int. J. Remote Sens.,* 25, 4051–4059. DOI: 10.1080/01431160310001657498.

Levy, R.C., Remer, L.A., Tanre', D., Matoo, S. & Kaufman Y.J. (2009). *Algorithm for remote sensing of tropospheric aerosol from MODIS: Collection 005 and 0.51*. http://modis-atmos.gsfc.nasa.gov

Li, R.R., Kaufman, Y.J., Gao, B.C. & Davis C.O. (2003). Remote sensing of suspended sediments and shallow coastal waters. *IEEE Transactions on Geoscience Remote Sensing*, 41, 559–566. DOI:10.1109/TGRS.2003.810227.

Matsushita, B., Yang, W., Chang, P., Yang, F. & Fukushima T. (2012). A simple method for distinguishing global Case-1 and Case-2 waters using SeaWiFS measurements. *ISPRS Journal of Photogrammetry and Remote Sensing,* 69, 74–87. DOI:10.1016/j.isprsjprs.2012.02.008.

May, C.L., Koseff, J.R., Lucas, L.V., Cloern, J.E. & Schoellhamer D.H. (2003). Effects of spatial and temporal variability of turbidity on phytoplankton blooms. *Mar. Ecol. Prog. Ser.,* 254, 111–128. DOI:10.3354/meps254111.

Mayer, L.M., Keil, R.G., Macko, S.A., Joye, S.B., Ruttenberg, K.C. & Aller R.C. (1998). Importance of suspended particulates in riverine delivery of bioavailable nitrogen to coastal zones. *Global Biogeochemical Cycles,* 12, 573–579. DOI:10.1029/98GB02267.

Miller, R.L. & McKee B.A. (2004). Using MODIS Terra 250 m imagery to map concentrations of total suspended matter in coastal waters. *Remote Sens. Environ.,* 93, 259–266. DOI:10.1016/j.rse.2004.07.012.

Min, J.E., Ryu, J.H., Lee, S. & Son S. (2012). Monitoring of suspended sediment variation using Landsat and MODIS in the Saemangeum coastal area of Korea. *Mar. Pollut. Bull.,* 64, 382–390. DOI:10.1016/j.marpolbul.2011.10.025.

Morel, A. & Bélanger S. (2006). Improved detection of turbid waters from ocean color sensors information. *Remote Sens. Environ.,* 102, 237–249. DOI:10.1016/j.rse.2006.01.022.

Olsen, C.R., Cutshall, N.H. & Larsen I.L. (1982). Pollutant–particle associations and dynamics in coastal marine environments: a review. *Mar. Chem.,* 11, 501–533. DOI:10.1016/0304-4203(82)90001-9.

Ramaswamy, V., Rao, P.S., Rao, K.H., Thwin, S., Rao, N.S. & Raiker V. (2004). Tidal influence on suspended sediment distribution and dispersal in the northern Andaman Sea and Gulf of Martaban. *Marine Geology,* 208(1), 33–42. DOI:10.1016/j.margeo.2004.04.019.

Salomonson, V. & Appel I. (2006). Development of the Aqua MODIS NDSI fractional snow cover algorithm and validation results. *IEEE Transactions on Geoscience Remote Sensing*, 44, 1747–1756. DOI:10.1109/TGRS.2006.876029.

Shi, W. & Wang M. (2007). Detection of turbid waters and absorbing aerosols for the MODIS ocean color data processing. *Remote Sens. Environ.,* 110, 149–161. DOI:10.1016/j.rse.2007.02.013.